At the thought of statistics, the Collector, walking through the chaotic Residency garden, felt his heart quicken with joy.... For what were statistics but the ordering of a chaotic universe? Statistics were the leg-irons to be clapped on the 'thugs' of ignorance and superstition which strangled Truth in lonely byways.

J.G. Farrell, The Siege of Krishnapur

Chapter 6

Integrated Visualization of Functional and Anatomical Brain Data: A Validation Study

Abstract

2D SPECT display and three methods for integrated visualization of functional and anatomical data are evaluated by a multi-observer study. **Methods:** SPECT and MRI data of 30 patients are presented using four types of display, *viz.* one of SPECT in isolation, two integrated 2D displays, and one integrated 3D display. Cold and hot-spots are pre-selected and indicated on printed black-and-white images of the data. Nuclear medicine physicians are asked to assign these spots to a lobe and a gyrus, and give a confidence rating for both localizations. Inter-observer agreement using kappa statistics and average confidence ratings are assessed to interpret the reported observations. **Results:** Both the inter-observer agreement and the confidence of the observers is larger for the integrated 2D displays than for the 2D SPECT display. A further increase in agreement and confidence is witnessed with the integrated 3D display. **Conclusions:** Integrated display of SPECT and MR brain images provides improved localization of cerebral blood perfusion abnormalities in relation to the anatomy of the brain over single modality display and increases the confidence of the observer.

6.1 Introduction

Integrated visualization is aimed at the efficient presention of information from different sources, usually combining a functional modality (SPECT, PET, fMRI) with an anatomical modality (CT, MRI). Correlation of functional processes with anatomical structures is hampered by the low spatial resolution of functional imaging modalities (Mazziotta and Koslow 1987, Kundel 1990, Zubal et al. 1995, Evans et al. 1996). These modalities might benifit from additional anatomical information provided by MRI and/or CT (see also (Levin et al. 1989, Holman et al. 1991, Valentino et al. 1991, Viergever et al. 1992, Hill et al. 1992, Britton 1994)).

In Chapters 3 and 4 several known and novel techniques have been proposed for integrated visualization of functional and anatomical brain images. This chapter presents a multi-observer study to evaluate three of these techniques, two for 2D and one for 3D display, so as to establish whether integrated visualization improves diagnostic agreement over single modality display. The diagnostic task for this study is the localization of cold and hot-spots in the cortex of the brain. We focus on the fusion of HMPAO–SPECT and T1-weighted 3D gradient-echo MR images of the brain, which have previously been registered.

We first present a brief overview of integrated visualization techniques, divided into 2D and 3D approaches.

6.1.1 Integrated 2D Visualization

Adjacent display of 2D images of different sources beit on a lightbox or a computer monitor can be considered the most rudimentary form of integrated visualization. A valuable extension of this approach is the use of a linked cursor indicating corresponding locations in several images (Hawkes et al. 1990) (see Figure 6.1*A* and *B*).

Integration of information from two or more image slices into one 2D image has been performed using alternate pixel display, color integration procedures, additional dimensions (height and time), areas and contours (Schad et al. 1987, Weiss et al. 1987, Pelizzari et al. 1989, Hawkes et al. 1990, Condon 1991, Viergever et al. 1992) (Chapter 3). Two categories can be distinguished, *viz.*; *i)* non-selective integration, where all information from the images, whether relevant or not, is combined using techniques such as multiplication, addition, or color scaling, and *ii)* selective integration, where specific diagnostic features (*e.g.*, regions, object boundaries, intensity ranges) are extracted and subsequently integrated into the display of another modality with the objective to optimally convey only the relevant information required to perform the diagnostic task (see Figure 6.1*C*).

Previous studies on non-selective integration of SPECT and MRI data showed that this approach conveyed little additional information, if at all, compared to adjacent display. Moreover, valuable features may be camouflaged by non-diagnostic

information (see Chapter 3). Consequently, while these techniques are easy to use and allow fast visualization, they are not effective. Color models hold more promise as the human visual system employs color more effectively than grey levels (Kundel 1990, Alfano et al. 1992, Stapleton et al. 1994). The HSV color model yields encouraging results, but the RGB model is not satisfactory for SPECT/MRI integration (Chapter 3).

Selective integration of SPECT and MRI data allows a more effective display of the relevant information. Initially the cost of segmentation was the main handicap, but in the past few years semi-automated segmentation methods to extract the brain from T1-weighted MR images have become available, *e.g.*, Höhne and Hanson (1992), Robb and Hanson (1996), Vincken et al. (1997), and Niessen (1997). Under well controlled circumstances, fully automatic extraction of the cerebral cortex has even appeared feasible (see Chapter 2).

6.1.2 Integrated 3D visualization

Integrated 3D visualization of functional and anatomical brain data includes windows (Levin et al. 1989, Hu et al. 1990) (Chapter 3), cutplanes (Evans et al. 1996) (Chapter 3), opacity weighted display (Evans et al. 1996), and surface mapping techniques (Levin et al. 1989, Hu et al. 1990, Payne and Toga 1990) (Chapter 4).

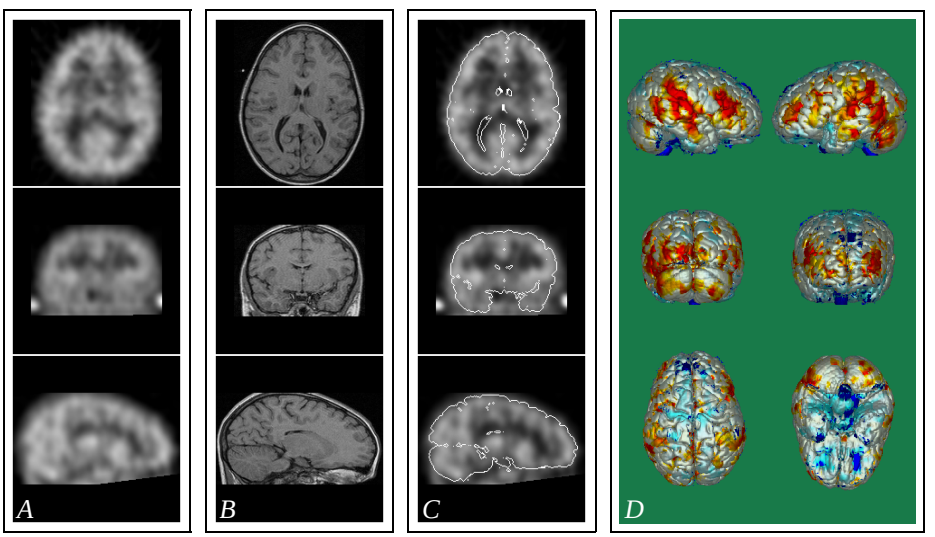

Figure 6.1 *The three integrated displays used for validation of the localization task. The 2D images of the datasets could be investigated with three orthogonal views (coronal, sagittal and transversal) and a cross-hair could be used to determine the location of a given point. Frame (A) and (B) show the 2D Adjacent display of (registered) SPECT images with corresponding MRI slices and Frame (C) shows the 2D Contour display. The Normal Fusion images in Frame (D) show renderings from six orthogonal directions.*

Furthermore, an integrated 3D presentation can be focussed on the visualization of already detected abnormalities (Wowra et al. 1989, Evans et al. 1996), so that standard volume visualization techniques can be applied (Wallis 1992).

In previous work we experimented with several of these techniques and found especially the Normal Fusion approach (Chapter 4 and Figure 6.1*D*) promising. A preliminary clinical evaluation of the Normal Fusion technique was conducted, which indicated that anatomical localization and communication might benefit from this technique. It was concluded that a thorough evaluation was required to establish whether simultaneous display of SPECT and MRI indeed offers increased diagnostic agreement among raters; this is the subject of the present study.

6.2 Materials and methods

We investigated the value of additional anatomical information for the localization of functional processes in the brain. Three techniques for integrated visualization of SPECT and MRI data were evaluated.

Cold and hot-spots in the cortical areas of clinical brain SPECT data were preselected and indicated on paper using black-and-white images (see Figure 6.2). Five nuclear medicine physicians were asked to assign these spots to the anatomy using four different types of presentation (see Figure 6.1), *viz.*; *i)* 2D SPECT display, *ii)* adjacent 2D display, *iii)* (selectively) integrated 2D display using the MRI brain contour, and *iv)* integrated 3D display using Normal Fusion. We verified that the location of the indicated abnormalities was identical in all display types. The cold and hot-spots had to be assigned to a lobe and a gyrus for all display types, and confidence had to be rated on a scale of 1 (very confident) to 5 (no confidence) for each localization. For each of the display types the inter-observer agreement was used as a measure for localization accuracy and the confidence values were averaged over all observations. Viewing conditions were identical to the clinical situation.

Three patient cases had been used in a training session prior to this localization study in order to familiarize the observer with the setup and anatomical information. These cases had already been used in a previous study (Chapter 4) and three of the five observers had worked with these training data at that time.

6.2.1 Patient data

Patient material was gathered by listing all patients with appropriate HMPAO–SPECT and MRI brain scans. A total of 30 patient datasets were selected from this list by the principal author (not a rater) where absence of gross abnormalities in both SPECT and MRI data was used as selection criterion. All 30 cases were acquired under the instruction of the Department of Child Psychiatry. Most of them (N=25) were diagnosed with Gilles de la Tourette Syndrome and/ or Attention-Deficit Hyperactivity Disorder and/ or comorbid disorders, the others (N=5) were diagnosed with disorders

such as autistic behavior and obsessive compulsive disorder. The nuclear medicine physicians were only supplied with the image data, no information concerning the patients could be consulted.

T1-weighted 3D gradient-echo MR images were acquired with a whole-body Philips Gyroscan 0.5 Tesla using a standard head coil. The acquisition data of the whole head consisted of contiguous axial slices of 1.2 mm thickness with TR=30 ms, TE=13 ms, 256×256 matrix, and 230 mm FOV. The SPECT image data were acquired with a Picker PRISM^{TM} three-detector gamma camera using a long-bore ultra high resolution, low energy fanbeam collimator and reconstructed to contiguous axial slices with a 64×64 matrix, a slice thickness of approximately 7.1 mm and a plane resolution of 7.5 mm FWHM.

6.2.2 Registration

One of the prerequisites for integrated visualization is adequate registration of the modalities. Registration is the process whereby the transformation matrix is calculated that relates the coordinate systems of different datasets. Earlier techniques involved frames or markers which were attached to the patient while acquiring the data. Nowadays, automated, retrospective techniques are becoming available (Maintz and Viergever 1998).

The required registration was performed using the Mutual Information technique (Maes et al. 1997). This automatic, robust, retrospective registration technique maximizes the statistical dependence between image intensities of voxel pairs of different datasets, thereby calculating the required transformation matrix to align them geometrically. The determined matrix was applied to the SPECT data using cubic convolution (Parker et al. 1983), in effect resampling the SPECT data to the MRI data.

6.2.3 Segmentation

Another prerequisite is the segmentation of interesting structures that are to be visualized. Segmentation extracts meaningful objects from digital image data by grouping voxels into larger, basic structures. These structures can be used for quantitative measurements or for visualization purposes (*e.g.*, a 3D volume visualization of the brain). Different strategies are available for the extraction of objects from a dataset, such as manual drawing in 2D slices, thresholding, region growing, interactive methods using mathematical morphology, near-automatic methods based on multiresolution, or completely automatic brain segmentation using region growing and mathematical morphology (see Chapter 2). For an extensive overview on MRI brain segmentation we refer to Clarke et al. (1995).

In the present study, segmentation of the MRI datasets was performed using ANALYZE™ (Robb and Hanson 1996) based on region growing and mathematical morphology as described in (Höhne and Hanson 1992). The segmentation starts by ap-

plying a threshold range to the MRI dataset to determine a base volume encapsulating the brain. From this base volume the brain is extracted with a sequence of erosion, region growing around a seed point in the brain, and geodesic dilation with the base volume as a mask. Using ANALYZE™ a satisfactory segmentation of the brain was performed in 15 minutes. The segmented brain was used for the Normal Fusion visualizations and for defining the brain contours in transverse MRI slices; these contours were subsequently superimposed onto the corresponding registered SPECT images for integrated 2D display (see Figure 6.1*C*).

6.2.4 Display methodology

We evaluate the value of integrated visualization over single modality SPECT display. The basis for the latter is the routine viewing of SPECT data at the Nuclear Medicine department, supported by the reporting and image manipulation program MedView™. Multiplanar 2D images can be displayed along the three orthogonal axes of the volume data and a cross-hair can be used to determine the 3D position of a given location. A mouse click in one of the images updates the other orthogonal images to the indicated position. Furthermore, a color lookup table can be chosen and changed at will by the observer.

Three integrated visualization techniques were used for the validation study (see Figure 6.1), *viz.*; *i)* integrated 2D visualization with adjacent display (denoted as 2D Adjacent), *ii)* integrated 2D visualization with selective integration of contours of the brain from MRI superimposed onto the SPECT data (denoted as 2D Contour), and *iii)* integrated 3D visualization using images rendered with the Normal Fusion technique of the SPECT/MRI data (in the remainder of this chapter referred to as 3D Normal Fusion). The visualization techniques which were used in this validation study have been described in Chapters 3 and 4, and will be only briefly reviewed here.

For the contours from the MRI data superimposed onto the SPECT images we used a value corresponding to the maximum SPECT value, in effect assigning the highest lookup table color (usually white) to the contours.

With the 3D Normal Fusion technique local functional information is sampled and projected onto an anatomic structure along a path defined by the inward normal of the local surface direction (Chapter 4). In the present study the SPECT data below the cortical surface were sampled in the range [0 - 15 mm]. The average value was subsequently color encoded onto the MRI cortex rendering, so as to signal both cold and hot-spots. The observers were supplied with one image containing six orthogonal 3D Normal Fusion visualizations of the brain under investigation (see Figure 6.1*D*).

Assignment of a lookup table for color encoding of the 3D Normal Fusion images is very difficult as use of color is dependent on the operator, the monitor, and the environment, which makes a general consensus for the optimum table nigh impossible to obtain. This is why a technique described in Chapter 5 was used that enables the observer to manipulate control points for the color lookup table of the functional

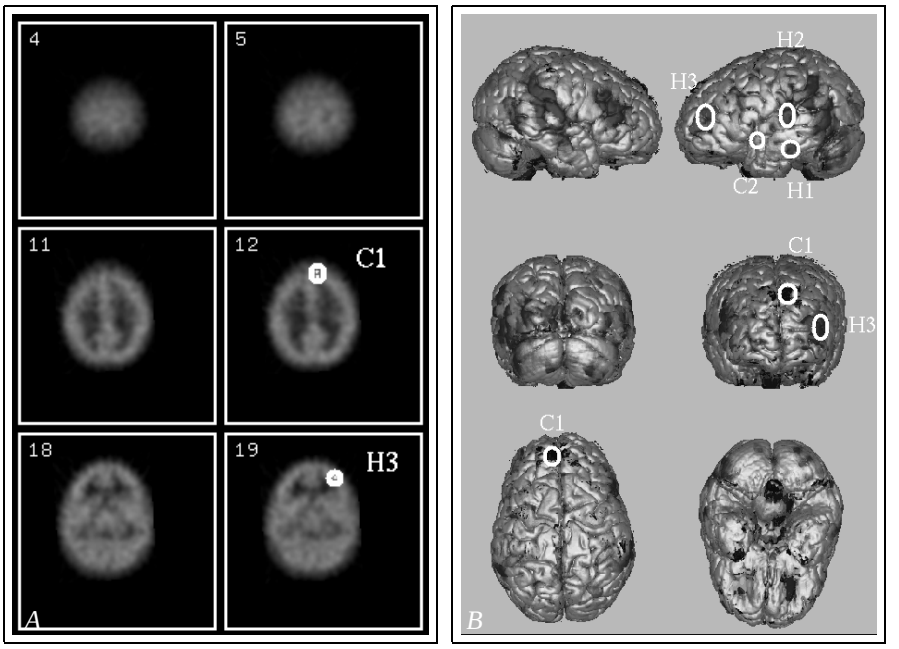

Figure 6.2 *Selection of printed images used to indicate pre-selected cold (C1 and C2) and hot-spots (H1, H2, H3) to be localized.*

information of the 3D Normal Fusion visualizations.

6.2.5 Setup

The localization task for the four display types (see Figure 6.1) was performed by five nuclear medicine physicians in their usual setting. The patient cases were randomized for each display type. Complete randomization over all display types was impractical as observers would have to switch between different displays and monitors. Furthermore, an undesirable memory effect would have been introduced, *i.e.*, we had experienced from the training session that the 3D Normal Fusion images make it easy to remember certain spots. The incomplete randomization possibly introduces a learning effect, but this should be minimized by the training session.

The spots to be localized with the 2D displays were indicated on paper by using a printed black-and-white image of the (registered, for the 2D Adjacent and 2D Contour display) SPECT slices with a superimposed circle and code that consisted of a C for cold-spots, an H for hot-spots and a number (see Figure 6.2*A*). The 3D Normal Fusion display was presented as a printed black-and-white image of the six visualizations with superimposed circles and the codes corresponding to the codes in the SPECT display (see Figure 6.2*B*).

The localization was restricted to cold and hot-spots in the cortical surface layer;

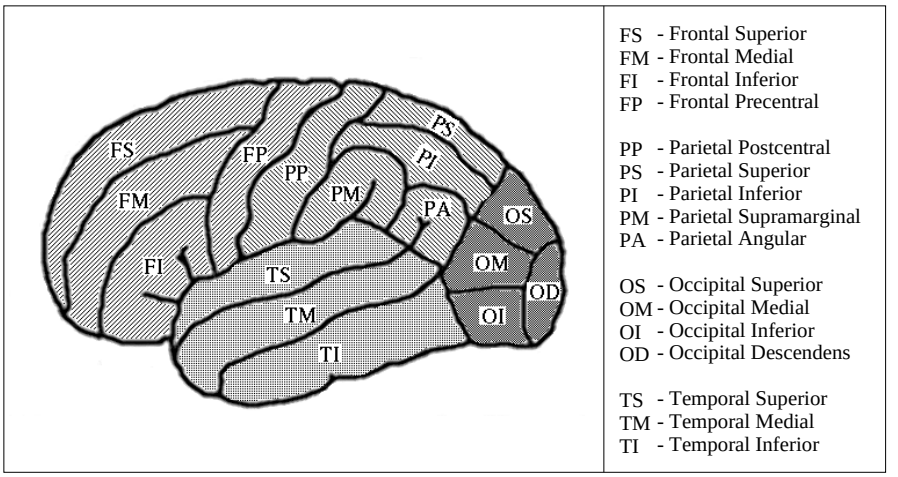

Figure 6.3 *A schematic subdivision of the brain in lobes and gyri for the localization of abnormalities.*

the 3D Normal Fusion technique is not suitable for the presentation of functional information in other parts of the grey matter. To avoid ambiguities in the localization of the patient data, only focal spots were used (spots that span an area may cause problems in assignment to a specific lobe or gyrus). A total of 122 spots resulted in 122 $\times$ 5 raters $\times$ 4 displays = 2440 observations, consisting of a lobe and gyrus localization and a confidence rating for both.

The location of a cortical spot had to be assigned to a lobe (frontal, parietal, occipital, temporal), and gyrus (*e.g.*, superior temporal gyrus). The observers were supplied with the atlasses of Duvernoy (1991), Kahle et al. (1995), and Gray (1994) for reference on brain anatomy and a schematic summary was supplied (see Figure 6.3). Both localization aspects had to be rated with a confidence measure ranked as follows: 1 = very confident, 2 = confident, 3 = reasonably confident, 4 = low confidence, 5 = no confidence. Statistical evaluation was performed using a kappa (κ) value for inter-observer variability on localization and an average value for confidence.

6.2.6 Statistical analysis

Inter-observer agreement for two raters can be assessed using the κ-value, originally proposed by Cohen (1960), which represents agreement corrected for chance agreement. Since then several investigators have evaluated and improved this measure for different statistical purposes. For this study we used the κ-value proposed by Fleiss (1971) to deal with data from more than two raters (see Formula (6.1)). A κ-value is 1.0 when the agreement between observers is perfect and 0.0 when it is not different

from chance agreement (Mezzich et al. 1981). Landis and Koch (1977) ranked the κ-value as follows: Lower than 0.00 poor agreement; 0.00 - 0.20 slight agreement; 0.21 - 0.40 fair agreement; 0.41 - 0.60 moderate agreement; 0.61 - 0.80 substantial agreement; and 0.81 - 1.00 almost perfect agreement.

$$\kappa = \frac{\sum_{a=1}^{n}\sum_{\substack{b=1 \\ b\neq a}}^{n}(1-P_{a,b})\kappa_{a,b}}{\sum_{a=1}^{n}\sum_{\substack{b=1 \\ b\neq a}}^{n}(1-P_{a,b})} \quad with: \quad \kappa_{a,b} = \frac{P_i - P_{a,b}}{1-P_{a,b}} \quad 95\%CI = \kappa \pm 1.96 * sd_\kappa \tag{6.1}$$

Equation 6.1 expresses the κ-value over all observers, which is a weighted average of the κ-values over all observer pairs ($\kappa_{a,b}$). $P_{a,b}$ is the expected proportion of agreement between the ath and the bth observer under the null hypothesis of independence, *i.e.*, chance agreement. P_i is the observed proportion of agreement between two observers. The 95% confidence interval (95%*CI*) is calculated from the standard deviation (*sd*) over all $\kappa_{a,b}$ calculations. For details we refer to Fleiss (1971). The κ-value and 95%*CI* were calculated using Agree 5.0 for computing agreement on nominal data (R. Popping, iecProGamma, Netherlands 1989).

The confidence ratings for the lobar and gyral localization for each of the four display types were calculated using an arithmetic mean over all observations.

6.3 Results

In Table 6.1 the final results over all measurements are presented for each of the display types. The first row presents the results for the 2D SPECT display, row 2 the results for 2D Adjacent display, row 3 the 2D Contour display, and row 4 the 3D Normal Fusion display. The columns are divided into two parts for anatomical localization, *i.e.*, the lobes and gyri. Each localization part is subdivided into a κ-value with 95%*CI*, and an average measure of perceived confidence in the localization given.

	Lobe		**Gyrus**	
	$\kappa \pm 95\%CI$	confidence	$\kappa \pm 95\%CI$	confidence
2D SPECT	0.74 ± 0.03	1.6	0.32 ± 0.02	2.8
2D Adjacent	0.84 ± 0.03	1.3	0.40 ± 0.02	2.4
2D Contour	0.84 ± 0.03	1.3	0.38 ± 0.02	2.4
3D Normal Fusion	0.86 ± 0.03	1.2	0.54 ± 0.02	2.0

Table 6.1 *Results for the lobar and gyral localization of cold and hot-spots. Inter-observer correspondence is expressed as a κ-value with 95%CI, and an average confidence measure is calculated for the four display settings.*

The results show that the κ-value measuring observer agreement for anatomical localization increases when anatomical information from MRI is added to the SPECT information. There is no difference between the 2D Adjacent and 2D Contour display, but for gyral localizations the 3D Normal Fusion display is superior to both integrated 2D displays. The average confidence measure shows similar results, *i.e.*, the confidence of the observers in their localizations increases when additional anatomical information is supplied. Again, the 3D Normal Fusion display improves the confidence of the observers for gyral localizations.

6.4 Discussion

The κ and confidence values for lobar localizations are very high (see Table 6.1) which signifies a high accuracy for this task even for 2D SPECT display. Additional anatomical information from the integrated 2D displays improves the inter-observer agreement and confidence of observations. A significant further improvement can not be accomplished using 3D Normal Fusion. This suggests that the 2D Contour and 2D Adjacent display are sufficiently accurate for lobar localization. However, all observers noted that the localization was performed considerably faster with the 3D Normal Fusion display.

Due to the relatively low spatial resolution, gyral localization of abnormalities in SPECT images is difficult compared to the lobar localization, which explains the lower κ and confidence values. For this task, the 3D Normal Fusion display outperforms the other techniques appreciably and has a κ-value with acceptable accuracy.

Overall, the observers reported a strong appreciation for additional anatomical information, which they do not usually have available on screen. Especially the 3D Normal Fusion images were appreciated as a pleasant and fast method for localizing abnormalities. Some of the observers reported a preference for the 2D Adjacent display over the 2D Contour because the contours were considered annoying as they interfered with the SPECT data. However, the results indicate that the 2D Contour display is as effective as the 2D Adjacent display for localization of abnormalities. Furthermore, the adjacent display of images still requires mental integration by the observer. The addition of a linked cursor is helpful, but integrated images appear to alleviate overall screening even more. Also, the 2D Contour display requires loading of only one dataset into memory, with the 2D Adjacent display this is doubled. In addition, the viewing was performed on 8-bit color display monitors which caused a problem with the 2D Adjacent display. The use of color for SPECT in this display type implied that the MRI data were color encoded with the same lookup table, which is a problematic issue in clinical procedures. There are solutions to the 8-bit color problem, but these result in poorer image quality or higher cost. We consider the 2D Contour display to be at least as promising for integrated 2D display as adjacent presentation and an additional option to turn the contour on and off is expected to

resolve the initial criticism.

Further options were suggested by the evaluators. Especially a linked cursor for integrated 2D display and an extension to a 3D volume visualization of the brain was considered a desirable attribute (see also Section 3.3.2.1). Furthermore, the indication of specific features, *e.g.*, main sulci, is likely to improve localization abilities of observers in display types.

6.5 Conclusions

Fusion of SPECT and MRI information increases the ability of clinicians to localize abnormalities in the functional SPECT data, and increases confidence of their observations. Volumetric display using the 3D Normal Fusion technique has proven particularly efficient for this purpose.

The results indicate that abnormalities present in SPECT data can be localized with acceptable accuracy at the gyral level by supplying additional anatomical information. This finding opens up new possibilities for clinical procedures where precise localization of (cerebral) functional information is required.

Acknowledgements

We are indebted to our colleagues P.C. Anema, F.J. Beekman, B. Derksen, R.T.M. Jonk, C. Haring, R.M. Hoogeveen, J. Kervel, R. Maas, J.B.A. Maintz, L.C. Meiners, W.J. Niessen. We gratefully acknowledge the research licence of ANALYZE^{TM}, provided by Dr R.A. Robb, Mayo Foundation/ Clinic, Rochester, Minnesota.